

## *Artocarpus heterophyllus* Lam. Stem Bark Inhibits Melanogenesis through Regulation of ROS, cAMP, and MAPK Pathways

(*Artocarpus heterophyllus* Lam. Kulit Batang Merencat Melanogenesis melalui Pengawalaturan Laluan ROS, cAMP dan MAPK)

HAZWANI MAT SAAD<sup>1</sup>, CHUN HOE TAN<sup>2</sup>, SUGUMARAN MANICKAM<sup>3</sup>, SIEW HUAH LIM<sup>4</sup> & KAE SHIN SIM<sup>1\*</sup>

<sup>1</sup>*Institute of Biological Sciences, Faculty of Science, Universiti Malaya, Jalan Profesor Diraja Ungku Aziz, 50603 Kuala Lumpur, Federal Territory, Malaysia*

<sup>2</sup>*Department of Biotechnology, Faculty of Applied Science, Lincoln University, 47301 Petaling Jaya, Selangor Darul Ehsan, Malaysia*

<sup>3</sup>*Rimba Ilmu Botanical Garden, UM Sustainability Development Centre, Level 6, Research and Innovation Management Complex, Universiti Malaya, Jalan Profesor Diraja Ungku Aziz, 50603 Kuala Lumpur, Federal Territory, Malaysia*

<sup>4</sup>*Department of Chemistry, Faculty of Science, Universiti Malaya, Jalan Profesor Diraja Ungku Aziz, 50603 Kuala Lumpur, Federal Territory, Malaysia*

Received: 17 August 2022/Accepted: 23 November 2022

### ABSTRACT

Natural-based skin-lightening cosmeceutical products are attracting high popularity nowadays due to their relatively high bioavailability upon application. *Artocarpus* species have been highlighted with such potential, and our previous studies have reported that *Artocarpus heterophyllus* Lam. stem bark extract exhibited a potent anti-melanogenic activity by reducing melanin content and inhibiting cellular tyrosinase activity in B16F10 melanoma cells. Hence, this study aimed to identify the bioactive fraction from *A. heterophyllus* Lam. stem bark and determine its anti-melanogenic mechanisms in B16F10 melanoma cells. Our results showed that a fraction (H-3) demonstrated the most pronounced anti-melanogenic effect at 12.00 µg/mL by reducing melanin content to  $22.86 \pm 2.90\%$  and inhibiting cellular tyrosinase activity at treatment concentration 33-fold lower than kojic acid, without being cytotoxic against B16F10 melanoma cells. Moreover, treatment with H-3 for 24 and 48 h substantially scavenged intracellular reactive oxygen species (ROS) of hydrogen peroxide-challenged B16F10 melanoma cells by 1.8 and 4.4%, respectively. Based on the microarray profiling and qPCR analysis, H-3 downregulated *Creb3l1*, *Creb3l2*, *Creb3l3*, *Mitf*, *Tyr*, *Tyrp1*, and *Dct* genes in B16F10 melanoma cells, whereas the expression of *Map3k20*, *Mapk14* (p38), and *Foxo3* genes was markedly increased. Altogether, these results demonstrated that H-3 exhibited its anti-melanogenic activity in B16F10 melanoma cells through scavenging ROS and concurrent inhibition of the cAMP and activation of the p38/MAPK signaling pathways. These findings indicate that H-3 has the potential to be used as a skin lightening cosmeceutical agent in the treatment of skin hyperpigmentation.

Keywords: B16F10 melanoma cells; melanin; microarray profiling; microphthalmia-associated transcription factor; tyrosinase

### ABSTRAK

Produk kosmetik pencerah kulit berasaskan sumber semula jadi mempunyai kepopularan yang tinggi pada masa kini kerana bioketersediaannya yang tinggi apabila digunakan. Spesies *Artocarpus* telah diserlahkan dengan potensi sedemikian dan kajian kami yang terdahulu telah melaporkan bahawa ekstrak kulit batang *Artocarpus heterophyllus* Lam. menunjukkan aktiviti anti-melanogenik yang kuat dengan menurunkan kandungan melanin serta menghalang aktiviti tirosinase sel pada sel melanoma B16F10. Oleh itu, kajian ini bertujuan untuk mengenal pasti fraksi bioaktif daripada kulit batang *A. heterophyllus* Lam. dan menentukan mekanisme anti-melanogenesis dalam sel melanoma B16F10. Hasil menunjukkan bahawa fraksi H-3 menunjukkan kesan anti-melanogenik yang ketara pada 12.00 µg/mL dengan menurunkan kandungan melanin kepada  $22.86 \pm 2.90\%$  serta menghalang aktiviti tirosinase sel pada kepekatan 33 kali

ganda lebih rendah berbanding asid kojik tanpa kesan ketoksikan pada sel melanoma B16F10. Tambahan pula, rawatan dengan H-3 selama 24 dan 48 jam dapat menghapuskan spesies oksigen reaktif (ROS) intrasel daripada sel melanoma B16F10 yang dicabar dengan H<sub>2</sub>O<sub>2</sub> dengan ketara masing-masing sebanyak 1.8 dan 4.4%. Berdasarkan profil jujukan mikroarai dan analisis qPCR, H-3 menurunkan pengekspresan gen *Creb3l1*, *Creb3l2*, *Creb3l3*, *Mitf*, *Tyr*, *Tyrb1* dan *Dct* dalam sel B16F10, manakala pengekspresan gen *Map3k20*, *Mapk14* (p38), dan *Foxo3* telah meningkat dengan ketara. Secara amnya, keputusan ini menunjukkan bahawa H-3 menunjukkan aktiviti anti-melanogenesis dalam sel melanoma B16F10 dengan mengikis ROS intrasel dan pada masa yang sama menghalang laluan isyarat cAMP serta mengaktifkan isyarat laluan p38/MAPK. Penemuan ini menunjukkan bahawa H-3 berpotensi untuk digunakan sebagai agen kosmetik pencerah kulit dalam rawatan hiperpigmentasi kulit.

Kata kunci: Faktor transkripsi berkaitan mikroftalmia; melanin; profil mikroatur; sel melanoma B16F10; tirosinase

## INTRODUCTION

Melanin determines the skin color and it is synthesized in melanosome through a series of complex oxidation steps, with tyrosinase as the rate-limiting enzyme (Parvez et al. 2006). Although melanin is beneficial to human, an excess deposition of melanin pigments in the epidermis and/or dermis layer of skin caused hyperpigmentation, making the skin appear darker than the natural skin color and thereby negatively affect the aesthetics (Hwang et al. 2022). Examples of hyperpigmentation-related disorders are melasma, solar lentigines, ephelides (freckles), and post-inflammatory hyperpigmentation (Plensdorf & Martinez 2009). The high aggressiveness of instrumental approach (e.g., cryotherapy, chemical peels, and lasers) and adverse effects of common synthetic anti-melanogenic agents (e.g., kojic acid, hydroquinone, and arbutin) (Ko, Shrestha & Cho 2018; Plensdorf & Martinez 2009; Solano et al. 2006; Takizawa et al. 2004) have shifted the consumers' preference to natural origin skin-lightening cosmeceutical agents (Chaikul et al. 2017; Chiang et al. 2014; Zheng et al. 2023).

*Artocarpus heterophyllus* Lam. (Moraceae), commonly known as jackfruit, is distributed widely in tropical and subtropical regions of Asia. It is a large (10-15 m in height) evergreen tree and usually cultivated for its edible fruits (Nguyen et al. 2012; Prakash et al. 2009). Various parts of *A. heterophyllus* Lam. including the root, leaves, stem bark, and latex have been utilized in folkloric medicine to treat a number of ailments (diarrhoea, fever, cough, wound, and asthma) and skin problems (abscesses and dermatitis) (Jagtap & Bapat 2010; Prakash et al. 2009). Recent studies have also reported that secondary metabolites from *A. heterophyllus* exerted various biological activities, such as anti-cancer, anti-inflammatory (Morrison et al. 2021), cytoprotective, antioxidant (Li et al. 2021), anti-bacterial (Ramli et al.

2021), anti-fungal (Vázquez-González, Ragazzo-Sánchez & Calderón-Santoyo 2020), anti-viral (Fu et al. 2020), and anti-tyrosinase (Arung, Shimizu & Kondo 2006; Li et al. 2020). Our previous studies have provided preliminary insight into the anti-melanogenic and anti-oxidation activities of five ethanolic extract of *Actocarpus* species, including *A. heterophyllus* (Saad et al. 2021). It was demonstrated that the *A. heterophyllus* stem bark extract exhibited the most pronounced anti-melanogenic effects without significant toxicity to the B16F10 melanoma cell line. In agreement with our previous report, Arung, Shimizu and Kondo (2011) have also reported that the woody part of *A. heterophyllus* exhibited great potential to be developed as a skin lightening agent due to its strong inhibitory effect on tyrosinase. Nonetheless, the anti-melanogenic mechanisms of the *A. heterophyllus* stem bark extract in B16F10 cells remain elusive.

In continuation to our previous studies (Saad et al. 2021), we herein performed bioassay-guided fractionation of the ethanolic *A. heterophyllus* Lam. stem bark extract, followed by a mechanistic investigation. The active fraction of the extract was identified by performing cell viability and melanin content assays using B16F10 melanoma cells. The bioactive fraction was then selected for further analyses, including cellular tyrosinase assays, flow cytometry, microarray profiling, and qPCR analysis.

## MATERIALS AND METHODS

### CHEMICALS AND REAGENTS

All chemicals were acquired from Sigma-Aldrich except for resazurin which was acquired from Bio-Rad Laboratories. ROS detection kit was acquired from Promokine. The microarray slides, qPCR consumables, and RNA isolation kit were acquired from Agilent Technologies.

## PLANT MATERIALS

Stem bark of *A. heterophyllus* Lam. was collected from Rimba Ilmu Botanical Garden, Institute of Biological Sciences, Faculty of Science, Universiti Malaya, Kuala Lumpur, Malaysia on 28<sup>th</sup> June 2018. The plant was identified, and the plant name has been checked with <http://www.theplantlist.org/tp11.1/record/kew-2653982>. The voucher specimen of *A. heterophyllus* Lam. (KLU 49925) was deposited at the herbarium of the Institute of Biological Sciences, Faculty of Science, Universiti Malaya, Kuala Lumpur, Malaysia.

## EXTRACTION AND BIOASSAY-GUIDED FRACTIONATION

The overall bioassay-guided fractionation is demonstrated in Figure 1. Briefly, *A. heterophyllus* Lam. ethanolic stem bark extract (6.63 g) which was previously obtained (Saad et al. 2021) was partitioned with water and chloroform to yield water (1.46 g) and chloroform (2.67 g) sub-extracts. The sub-extracts were then assessed with cell viability and melanin content assays (Saad et al. 2021) using B16F10 melanoma cells at a treatment concentration of 0.78-25.00 µg/mL. The chloroform sub-extract, being the more active sub-extract was subjected to flash column chromatography (silica gel, 230-400 mesh) that eluted using hexanes-chloroform

(9:1, 1:1, 1:4), chloroform (100%), chloroform-methanol (1-20%), followed by ethanol to furnish 12 semi-pure fractions (fraction A-L, 500 mL each). The bioactivity assessments were conducted on these fractions by performing the above-mentioned assays at the same treatment concentration, and fraction H was then identified as the bioactive fraction. Fraction H (0.75 g) was therefore further purified using preparative radial chromatography (silica gel 60 PF<sub>254</sub>), and eluted using hexanes-diethyl ether (9:1, 4:1, 1:1, 2:3, 3:7, 1:9), diethyl ether (100%), diethyl ether-methanol (3-12%), followed by ethanol to yield five fractions (H-1-H-5, 40 mL each). Aside from the cell viability and melanin content assays, additional assays were performed on these fractions at a treatment concentration of 0.38-12.00 µg/mL.

## LIQUID CHROMATOGRAPHY-MASS SPECTROMETRY (LC MS/MS) ANALYSIS

The phytochemical analysis of H-3 was performed as previously reported by Pang et al. (2022).

## CELL CULTURE, CELL VIABILITY, MELANIN CONTENT, AND CELL TYROSINASE ASSAYS

The cell culture procedure of B16F10 murine melanoma cells and the assays were conducted as outlined previously

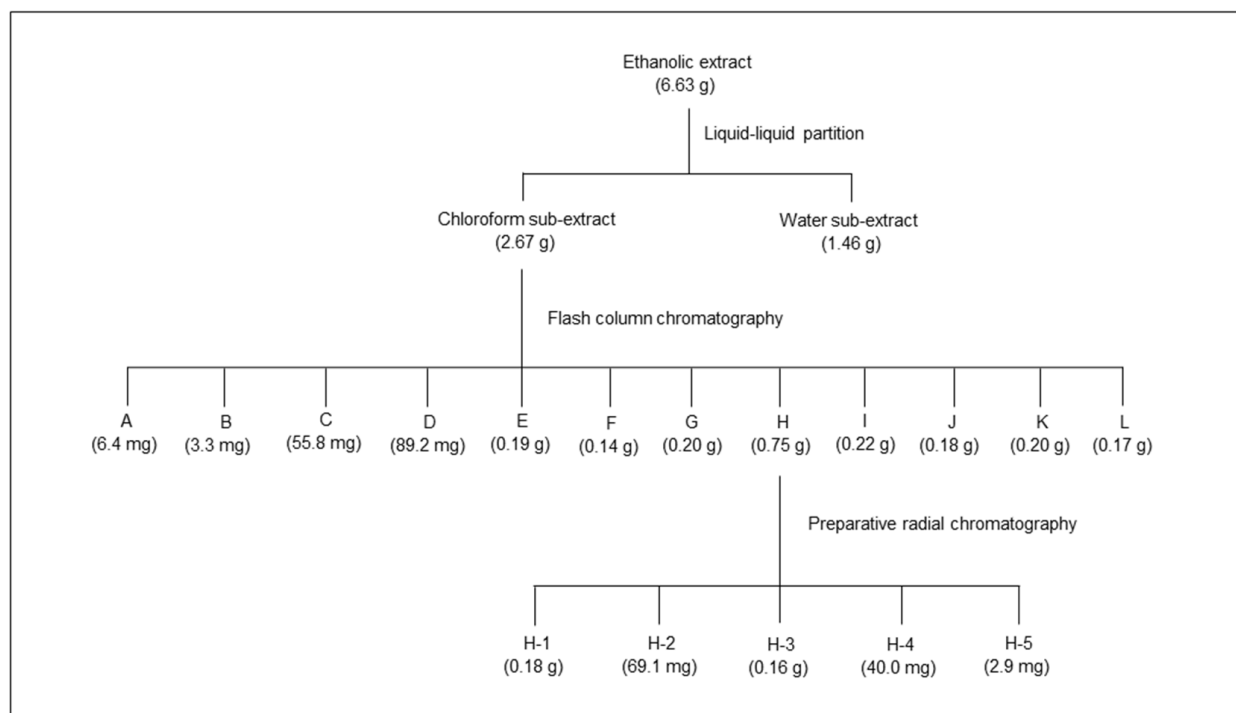


FIGURE 1. Fractionation of stem bark extract of *A. heterophyllus* Lam.

by Saad et al. (2021) with kojic acid as a positive control. The subsequent assays (flow cytometry, microarray profiling, and qPCR analysis) were conducted on the fraction that demonstrated the highest reduction of melanin content, strongest inhibition of cell tyrosinase activity, and least cytotoxic.

#### MEASUREMENT OF INTRACELLULAR REACTIVE OXYGEN SPECIES (ROS)

The intracellular ROS level in B16F10 melanoma cells was measured using flow cytometry according to the protocol outlined by Promokine ROS Detection Assay Kit, which utilized 2',7'-dichlorodihydrofluorescein diacetate as the fluorescence probe. In brief, cells were seeded with a density of  $1 \times 10^5$  cells/dish in a 60-mm cell culture dish. After incubated overnight, the cells were exposed to hydrogen peroxide ( $H_2O_2$ ) (20 mM) for 1 h, following by treatment with H-3 (12  $\mu$ g/mL) in the presence of  $\alpha$ -MSH (100 nM) for 24 and 48 h. Wells containing cells and  $\alpha$ -MSH without treatment were accounted as negative control, while those incubated with  $H_2O_2$  for 1 h and  $\alpha$ -MSH without treatment were used as positive control. After the designated treatment periods, the cells were washed with PBS twice, harvested, and resuspended in assay buffer provided by the kit at concentration of  $1 \times 10^6$  cells/mL, followed by incubation with 2',7'-dichlorodihydrofluorescein in the dark for 30 min at 37 °C. The fluorescence intensity of 2',7'-dichlorofluorescein was measured by a BD FACS Canto II flow cytometer and analyzed using a FACSDiva software. A total of  $1 \times 10^4$  events was collected.

#### TOTAL RNA EXTRACTION, MICROARRAY ANALYSIS, AND REAL-TIME PCR (qPCR)

The total RNA from treated (H-3, 12  $\mu$ g/mL) and untreated B16F10 melanoma cells, the microarray (Agilent SurePrint G3 Mouse Gene Expression Microarray v3, design ID: 072363) and the qPCR analysis were performed as previously described by Tan et al. (2022). The sequence of the primers and their amplicon sizes used are displayed in Supplementary Information 1. *Gapdh* was used as a reference gene for normalization. The qPCR experiments were carried out according to the MIQE guidelines (Bustin et al. 2009).

#### STATISTICAL ANALYSIS

All data were presented as the means  $\pm$  standard deviation of three independent experiments. Single comparison between the means of two groups was analyzed using Student's *t*-test. The statistical analysis was performed using the GraphPad Prism 7.0 software

(GraphPad Software). The values are considered statistically significant when  $p < 0.05$ .

## RESULTS

#### BIOASSAY-GUIDED FRACTIONATION OF *A. heterophyllus* Lam. Stem Bark Extract

The effect of water and chloroform sub-extracts (Figure 1) on cell viability and melanin content in B16F10 melanoma cells were examined and the results are presented in Figure 2(A). Chloroform sub-extract exerted a higher anti-melanogenic activity compared to water sub-extract as evident from a lower melanin content ( $36.67 \pm 7.75\%$ ) at a concentration of 25.00  $\mu$ g/mL without appreciable cytotoxicity (cell viability  $> 50\%$ ). Thus, the chloroform sub-extract was selected for further fractionation using silica gel flash column chromatography and produced 12 semi-pure fractions (A-L) (Figure 1). Owing to a minute amount of fraction A (6.4 mg) and B (3.3 mg), these fractions were not tested in bioassays. The anti-proliferative and anti-melanogenic activities of fractions C-L were investigated using the same assays, and the results of active fractions (H, I, and J) are presented in Figure 2(B), whereas the non-active fractions (C, D, E, F, G, K, and L) are presented in Supplementary Information 2. All fractions were not cytotoxic (cell viability  $> 50\%$ ), except for the fraction H ( $11.21 \pm 7.85\%$ ) and I ( $44.56 \pm 3.79\%$ ) at the highest concentration tested (25.00  $\mu$ g/mL). In the melanin content assay, fraction H recorded the lowest melanin content ( $27.49 \pm 0.52\%$ ) at a non-cytotoxic concentration of 12.50  $\mu$ g/mL, and it was therefore selected for further purification using preparative radial chromatography to obtain another five fractions (Figure 1). Fraction H-5 was not tested in biological assays due to its extremely low yield (2.9 mg). The anti-proliferative and anti-melanogenic effects of fractions H-1 to H-4 were assessed and the results are illustrated in Figure 2(C). All fractions H-1 to H-4 are not cytotoxic, with fraction H-3 recorded the lowest melanin content ( $22.86 \pm 2.90\%$ ) at the highest concentration tested (12.00  $\mu$ g/mL) and it was 4-fold better than kojic acid ( $93.26 \pm 3.23\%$ ). Hence, H-3 was selected for subsequent investigation.

#### THE EFFECT OF FRACTION H-3 ON CELLULAR TYROSINASE ACTIVITY

Fraction H-3 exerted significant inhibition on cellular tyrosinase activity in a dose-dependent manner, from  $74.47 \pm 3.78\%$  at treatment concentration of 6.00  $\mu$ g/mL to  $40.41 \pm 4.89\%$  at 12.00  $\mu$ g/mL (Figure 2(D)). Interestingly, the inhibition of cellular tyrosinase activity

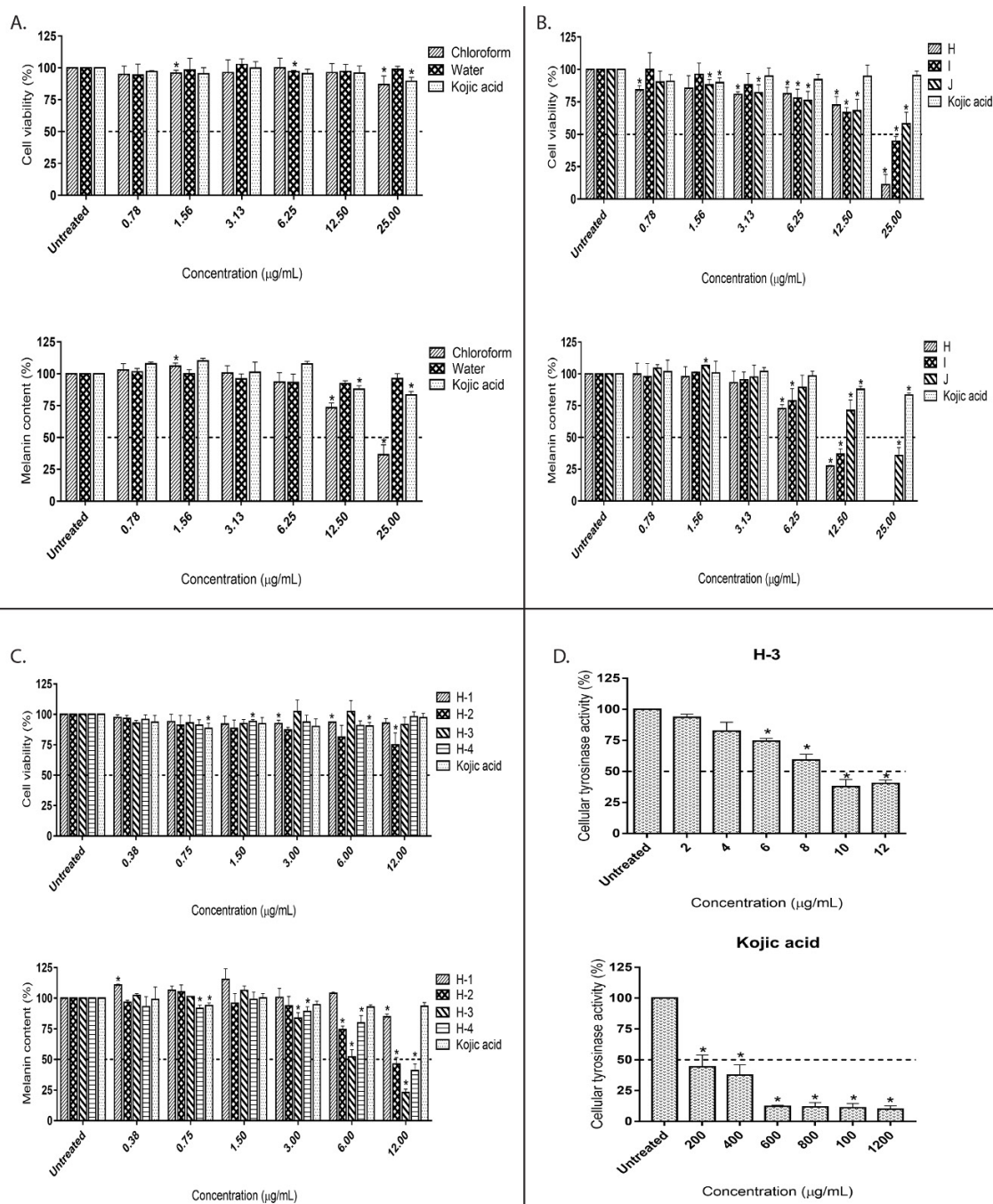


FIGURE 2. Viability and melanin content of B16F10 melanoma cells after treatment with *A. heterophyllus* Lam. stem bark (A) sub extract, (B) fractions (H–J), and (C) fractions (H-1–H-4) for 48 h. (D) effects of fraction H-3 and kojic acid on cellular tyrosinase activity. The concentrations of fractions that reduced  $\geq 50\%$  cell viability were excluded from the melanin content assay. Kojic

by fraction H-3 at 12.00  $\mu\text{g/mL}$  was similar to that of kojic acid ( $37.55 \pm 8.43\%$ ) at 400  $\mu\text{g/mL}$ , indicating that the former has reduced cellular tyrosinase activity at a treatment concentration 33-fold lower than kojic acid.

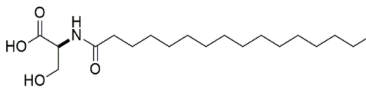
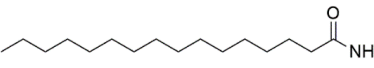
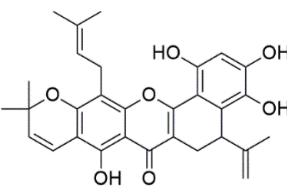
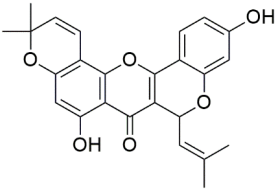
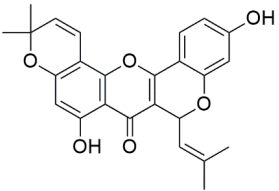
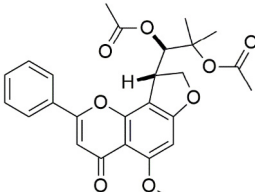
#### IDENTIFIED COMPOUNDS IN H-3

Based on the LC MS/MS analysis of H-3, six compounds have been identified based on Metlin database or Molecular Formula Generator algorithm with a score of

> 90% (deviation  $\pm 2$ ). Two of the identified compounds are fatty acids (N-palmitoyl serine and palmitic amide) and four are flavonoids (artonin B, cudraflavone A,

cyclomorusin, and polystachin). Table 1 summarized the identified compounds from H-3 through LC MS/MS analysis with reported bioactivities from literature.

TABLE 1. List of compounds present in H-3 based on LC MS/MS analysis

Class	Compound	Chemical structure	$m/z$ [M+H] <sup>+</sup>	Mass	Bioactivity	Reference
Fatty acid	N-palmitoyl serine (C <sub>19</sub> H <sub>37</sub> NO <sub>4</sub> )		344.2797	343.2718	Not reported	-
	Palmitic amide (C <sub>16</sub> H <sub>33</sub> NO)		256.2637	255.256	Not reported	-
Flavonoid	Artonin B (C <sub>30</sub> H <sub>30</sub> O <sub>7</sub> )		503.2077	502.2008	Anti-inflammatory activity by inhibiting superoxide anion generation in rat neutrophil cells	Wei et al. (2005)
					Cytotoxic against human CCRF-CEM leukemia cells by inducing apoptosis	Lee et al. (2006)
					Radical scavenging activity by inhibiting iron-induced lipid peroxidation in rat brain homogenate and copper-catalyzed oxidation of human low-density lipoprotein. Scavenged DPPH radical	Ko, Shrestha, S. & Cho (1998)
	Cudraflavone A (C <sub>25</sub> H <sub>22</sub> O <sub>6</sub> )		419.1485	418.1415	Anti-inflammatory activity by inducing	Wei et al. (2005)
	Cyclomorusin (C <sub>25</sub> H <sub>22</sub> O <sub>6</sub> )		419.1485	418.1415	Anti-inflammatory activity by inducing	Wei et al. (2005)
Anti-platelet activities in rabbit blood suspension					Lin et al. (1993)	
Anti-tyrosinase activity (mushroom tyrosinase)					Ryu et al. (2008)	
	Polystachin (C <sub>26</sub> H <sub>26</sub> O <sub>3</sub> )		467.1705	466.1634	Inhibited human phosphodiesterase-4 activity	Guo et al. (2018)
					Not reported	-

### THE EFFECT OF H-3 ON INTRACELLULAR ROS LEVEL

The reactive oxygen species (ROS) scavenging effect of H-3 in B16F10 melanoma cells are presented in Figure 3. Treatment with either  $\alpha$ -MSH or H-3 individually did not affect the ROS level in the cells (ROS level < 1%). The generation of ROS in the cells was induced by pre-

incubation with  $H_2O_2$  for 1 h prior to the treatment with H-3 for 24 and 48 h. The results showed that H-3 slightly reduced the intracellular ROS level from 2.5 to 1.8% after 24 h treatment. On the extension of the treatment to 48 h, H-3 further reduced the ROS level from 8.8 to 4.4%, indicative of a substantial ROS scavenging activity of H-3.

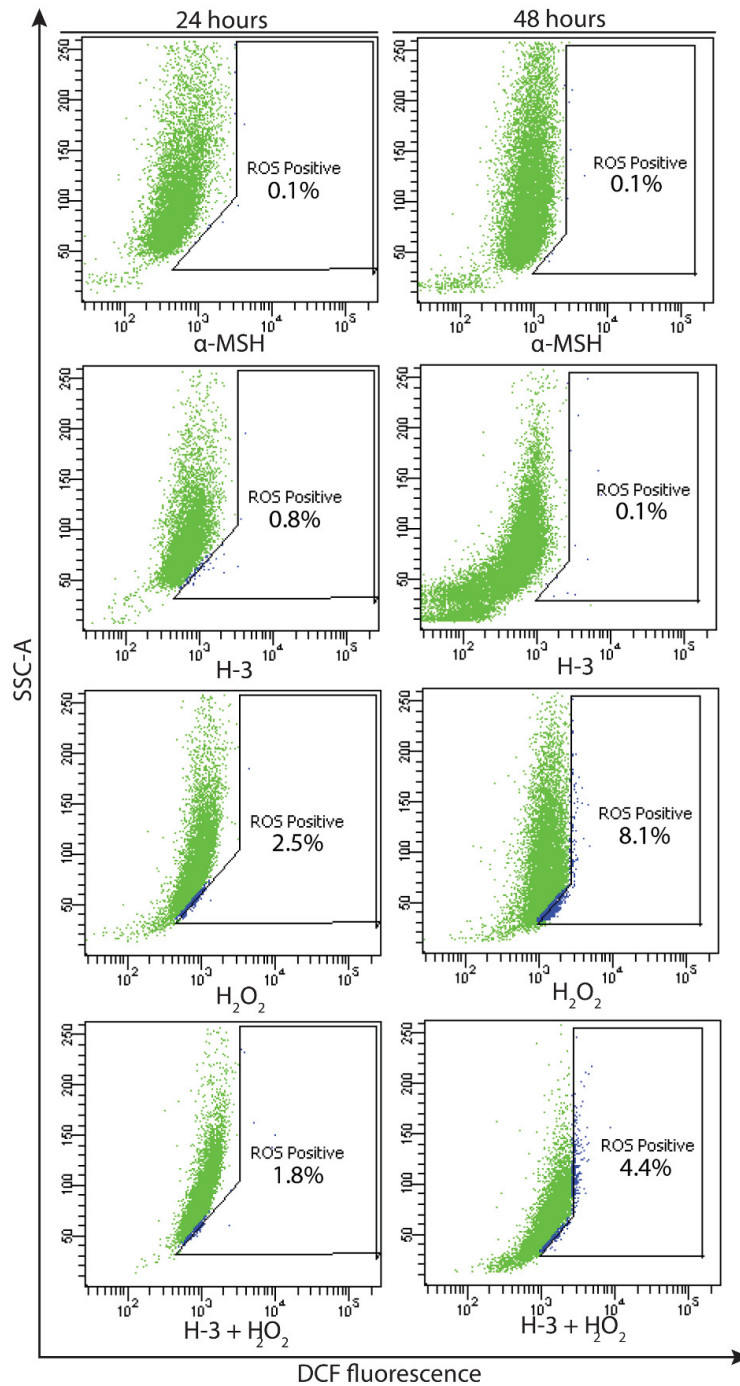


FIGURE 3. Effects of H-3 (12  $\mu$ g/mL) on intracellular ROS level in B16F10 melanoma cells after 24 and 48 h of treatment. Cells treated with medium containing  $\alpha$ -MSH only were regarded as a negative control, while those incubated with  $H_2O_2$  (20 mM) and  $\alpha$ -MSH were regarded as a positive control



THE EFFECT OF H-3 ON THE TRANSCRIPTOME IN B16F10  
MELANOMA CELLS

The transcriptome analysis in B16F10 melanoma cells showed that 4633 (14.62%) genes were differentially expressed upon treatment with H-3 at 12  $\mu\text{g}/\text{mL}$  at 48 h, out of 31700 that are present in the microarray (Figure 4(A)). Among these differentially expressed genes (DEGs), 1729 (5.45%) of them were upregulated, ranging from 2.00- to 16.95-folds, while 2904 (9.16%) of them were downregulated, ranging from 2.00- to 61.37-folds.

Through Gene Ontology, these DEGs can be grouped into three domains, namely biological process (BP), cellular component (CC), and molecular function (MF) (Figure 4(B)). The specific cellular events taken part by these DEGs in each domain were further elaborated and are presented in Figure 4(C1)–4(C3). Particularly, the DEGs involved in BP were subjected to further analysis, whereupon 29 genes that are related to melanogenesis were identified and are listed in Supplementary Information 3. Among these genes, the expression of a

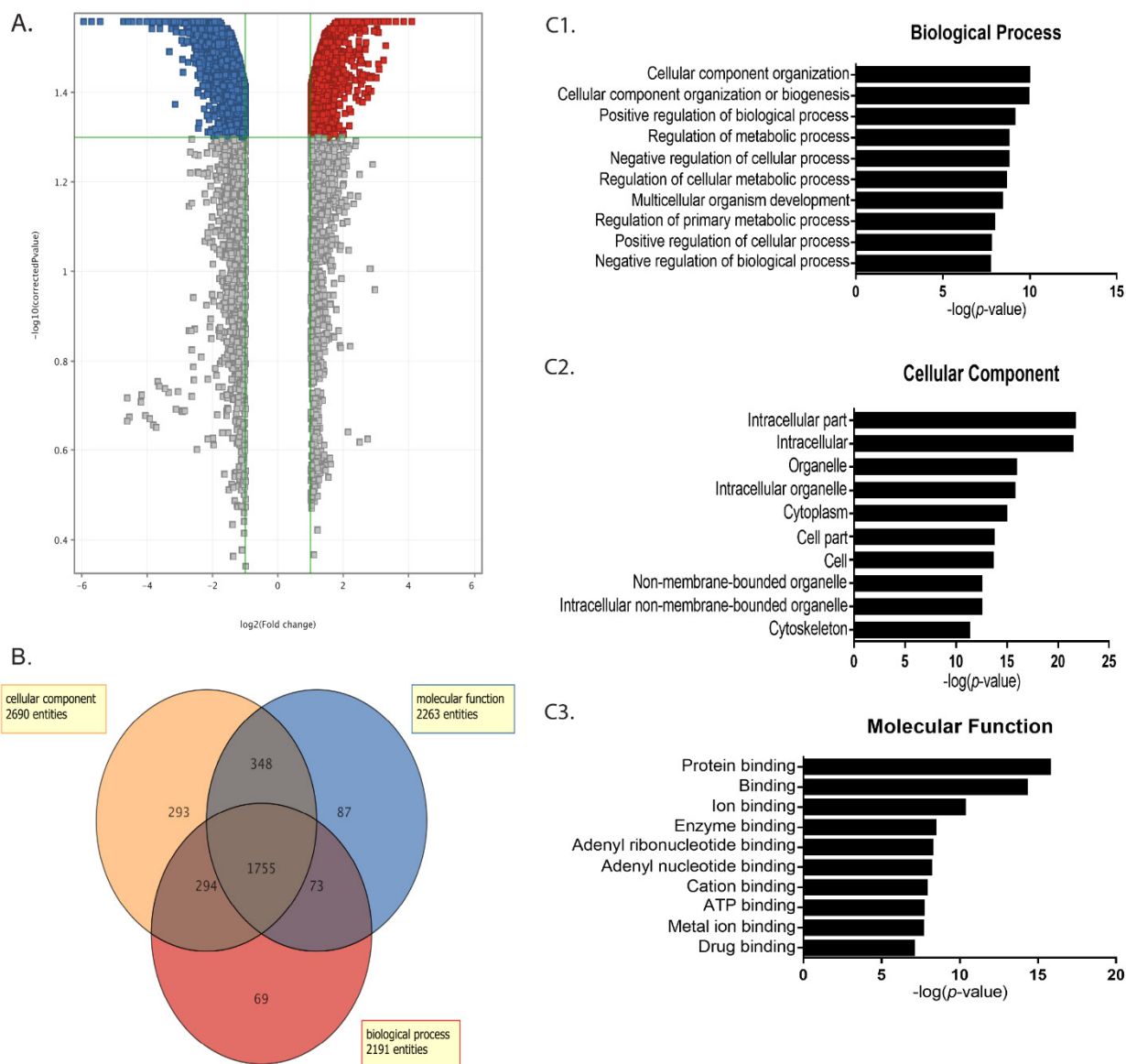


FIGURE 4. Microarray analysis of B16F10 melanoma cells treated with H-3 (12  $\mu\text{g}/\text{mL}$ ) for 48 h. (A) Volcano plot of DEGs after treatment with H-3. Each dot represents a gene. The red field represents the upregulated genes, and the blue field represents the downregulated genes with fold change  $> 2.0$  and  $p < 0.05$ . The grey coloured field represents the genes that do not meet the selection criteria, and they are non-DEGs. (B) Venn diagram shows the number of DEGs and their biological roles are classified into the biological process, cellular component, and molecular function. (C) Cellular events in B16F10 melanoma cells affected by H-3 based on GO analysis. (C1) Ten most significant biological process affected by H-3 treatment. (C2) Ten most significant cellular component affected by H-3 treatment. (C3) Ten most significant molecular function affected by H-3 treatment



master regulator of melanogenesis (*Mitf*), a rate-limiting enzyme in melanogenesis (*Tyr*), and a melanosome transport-associated gene (*Mlph*) were significantly downregulated by 2.69–6.78-fold. In addition, the markers of autophagy (involved in melanogenesis) were also significantly upregulated, such as *Sqstm1* and *Ulk1* (2.24-fold for both genes). The genes related to the cAMP signaling pathway, such as *Creb311*, *Creb312*, *Creb313*, and *Atf1* were downregulated by 2.10–3.58-fold. Furthermore, the genes involved in the MAPK signaling

pathway, i.e., *Map3k20* and *Mapk14* were upregulated by 4.10- and 2.01-fold, respectively.

The expression of selected DEGs involved in melanogenesis was validated using qPCR analysis and the results are shown in Figure 5. Treatment with H-3 for 48 h has significantly downregulated *Creb312*, *Creb313*, *Mitf*, *Tyr*, *Tyrp1*, and *Dct*; while *Map3k20* and *Mapk14* presented a significant increment in the expression level. The results of the qPCR analysis were therefore consistent with the microarray profile (Supplementary Information 3).

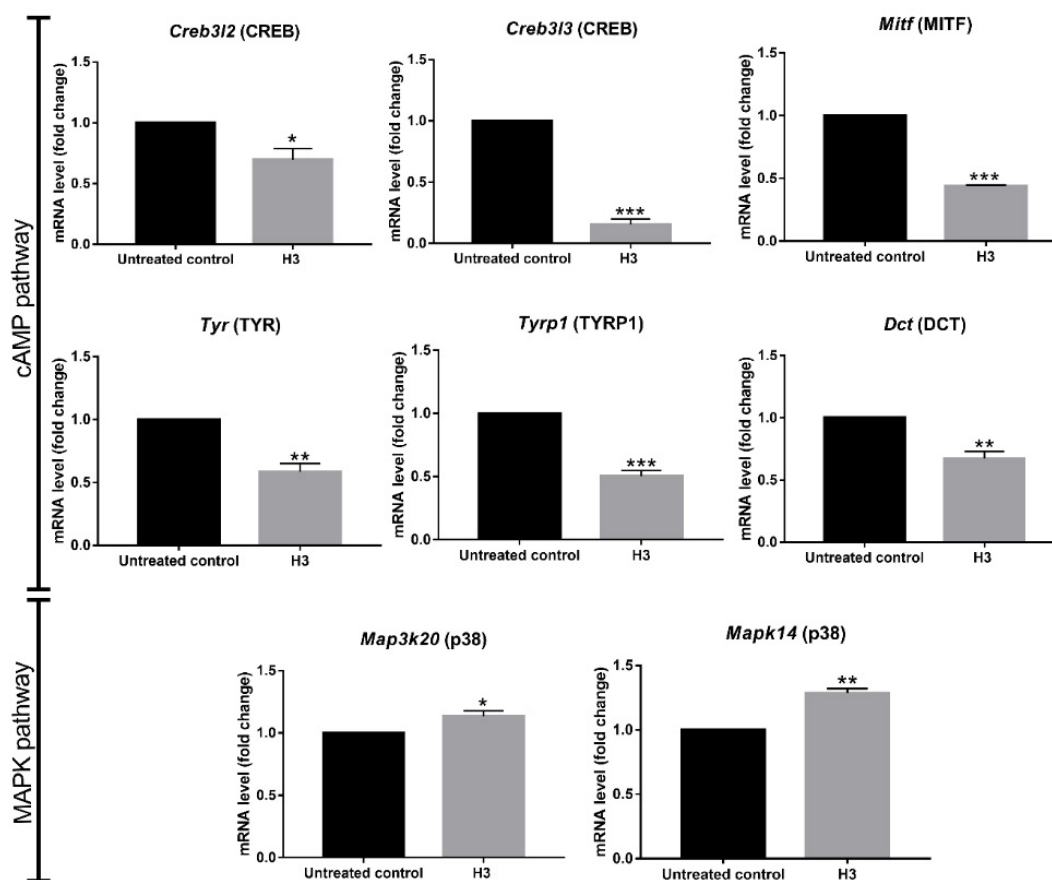


FIGURE 5. mRNA level of selected genes related to melanogenesis in B16F10 melanoma cells. mRNA level was examined using qPCR analysis. The  $2^{-\Delta\Delta C_q}$  method was employed to quantify the change in expression level between the untreated control and H-3 (12  $\mu\text{g}/\text{mL}$ ) cells and was based on the normalization with *Gapdh* (reference gene). The data are presented as the means  $\pm$  SD of three experimental observations (\* $p < 0.05$ , \*\* $p < 0.005$ , \*\*\* $p < 0.0005$ , multiple  $t$ -test)

#### DISCUSSION

Our previous screening on the anti-melanogenic activity of *A. heterophyllus* Lam. (Saad et al. 2021)

demonstrated that the stem bark extract exhibited a pronounced inhibitory effect on melanin production and cellular tyrosinase activity in B16F10 melanoma cells

without significant cytotoxicity. Hence, bioassay-guided fractionation of the extract was carried out in the current study. Prior to fractionation, proximate composition and pesticide residue testing was performed (Supplementary Information 4). It was found that *A. heterophyllum* Lam. stem bark extract contained a high amount of crude fibre (41.20%) and carbohydrate (33.20%), with a minute percentage of protein (2.20%) and crude fat (0.20%). Based on the pesticide residue analysis using GC/MS, the pesticide components, e.g., insecticides, rodenticides, fungicides, acaricides, and herbicides were not detected in the extract (Supplementary Information 5). A semi-pure fraction H-3 (Figure 1) was obtained through the bioassay-guided fractionation which potently reduced melanin content and inhibited cellular tyrosinase activity in B16F10 melanoma cells at concentration of 12 µg/mL. Based on the LC MS/MS analysis, three prenylated flavonoids including artonin B, cudraflavone A, cyclomorusin, and a flavone (polystachin) have been identified in H-3. These prenylated flavonoids were reported in the Moraceae family with several biological activities, including anti-tyrosinase effect (Table 1). Hence, it is tentatively suggested that these compounds which presented in H-3 might be contributed to the strong anti-melanogenic effect in B16F10 melanoma cells.

To further understand the anti-melanogenic mechanisms of H-3 in B16F10 melanoma cells, microarray profiling and qPCR analysis were performed. With all the gene expression results (Figures 4, 5 and Supplementary Information 3), the probable mechanisms of H-3 in B16F10 melanoma cells are outlined in Figure 6. Notably, H-3 treatment downregulated the expression of *Mitf*, a dimeric transcription factor that functions as a master regulator of melanogenesis, as well as a regulator of survival and differentiation of melanocytes (Bino Duval & Bernerd 2018; Levy, Khaled & Fisher 2006). This indicated that H-3 could have directly decreased the expression of *Mitf* gene that subsequently downregulated three crucial genes for melanogenesis, viz., *Tyr*, *Tyrp1*, and *Dct* (Sun et al. 2020) (Figure 6), leading to a decreased melanin content and inhibition of cellular tyrosinase activity in B16F10 melanoma cells.

The expression of MITF protein can be regulated transcriptionally through the cAMP signaling pathway (Price et al. 1998). Since our current study showed that H-3 treatment also decreased the expression of *Creb311*, *Creb312*, and *Creb313* genes (CREB), it is suggested that H-3 could have downregulated the *Mitf* gene in B16F10 melanoma cells through the inhibition of the cAMP/PKA signaling pathway. In addition, the *Atf1* gene (cAMP

dependant transcription factor, ATF-1) was downregulated upon H-3 treatment. ATF-1 is a crucial component in the cAMP signaling pathway, where the binding of this protein will activate CREB (Kawakami & Fisher 2017). The decreased *Atf1* gene expression and the ensuing inhibition of the cAMP/PKA signaling pathway have been observed in our studies, which are in accordance with those conducted by Roh et al. (2014) thus providing further verification that H-3 exhibited anti-melanogenic activity through the inhibition of this pathway.

Since treatment with H-3 has significantly increased the expression of *Map3k20* and *Mapk14* genes (p38) (Figure 5 and Supplementary Information 3), another hypothesized mechanism of H-3 is through the post-translational modification of MITF via ubiquitination (Alam et al. 2017; Wu et al. 2000) which involved the activation of the MAPK signaling pathway (Hsiao & Fisher 2014). Studies conducted by Ko et al. (2019, 2014) reported that eupafolin and *Annona squamosa* leaves extract have increased the expression of p38, subsequently leading to the manifestation of their anti-melanogenic activities. In addition to *Map3k20* and *Mapk14* genes (p38), H-3 also upregulated the expression *Uchl1os* gene (ubiquitin carboxyl-terminal hydrolase isozyme L1), indicating that H-3 reduced melanogenesis in B16F10 melanoma cells through the activation of the MAPK pathway, subsequently ubiquitinating the proteins involved in melanogenesis, such as MITF, tyrosinase, TYRP-1, and DCT in a proteasome-dependent mechanism (Figure 6) (Alam et al. 2018; Bellei et al. 2010).

The synthesized melanin in the melanosome will be transported to neighboring keratinocytes to distribute the melanin (Tsatmali, Ancans & Thody 2002). Aside from reducing melanin synthesis, H-3 could have interfered the melanosome transport, as downregulation of the genes involved in melanosome transport was detected, such as *Mlph* (Lee et al. 2018; Taira et al. 2018) and *Gpr143* (Makbal et al. 2020) (Supplementary Information 3). It has been reported that autophagy plays an important role in regulating melanogenesis by inducing melanosome degradation through autophagosomes (Jeong et al. 2020; Kim et al. 2020). In accordance with this, the markers for autophagy, such as *Sqstm1* (p62) and *Ulk1* (ULK1) were upregulated upon H-3 treatment for 48 h (Supplementary Information 3), suggesting that H-3 have probably activated autophagy and carried out melanosome degradation.

Reactive oxygen species (ROS) is a signaling molecule in the activation of the melanogenic pathway, hence, it is reasonable to suggest that scavenging ROS could be an effective approach to inhibit melanogenesis

(Ochiai et al. 2008). The effect of H-3 on intracellular ROS was analyzed using flow cytometry and the results showed that H-3 reduced ROS level in B16F10 melanoma cells that was previously elevated by H<sub>2</sub>O<sub>2</sub> (Figure 3). Kim et al. (2014) have shown that radical scavengers, such as vitamin C, N-acetylcysteine, and Trolox potentially inhibited melanogenesis in melanoma cells by activating Forkhead Box O3 transcription factor (FOXO3a), a regulator that involved in the antioxidative response in skin cells and other cell types. Additionally, Kwon et al.

(2017), reported that resveratrol, an anti-melanogenic agent exhibited ROS scavenging effect and induced the expression of FOXO3a protein in melanoma cells. In line with these studies, our microarray profile showed that H-3 significantly upregulated the expression of the *Foxo3* gene (Supplementary Information 3). Therefore, it can be hypothesized that the ROS scavenging ability of H-3 could be one of its anti-melanogenic mechanisms in B16F10 melanoma cells.

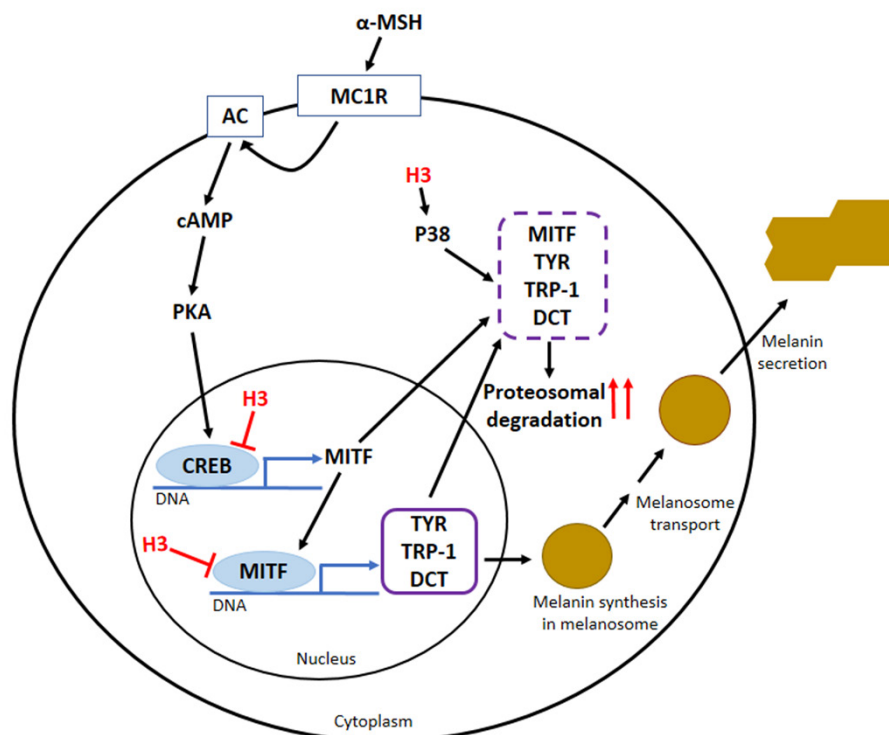


FIGURE 6. Putative anti-melanogenesis mechanisms of H-3 in B16F10 melanoma cells

#### CONCLUSIONS

In summary, the bioassay-guided fractionation of *A. heterophyllum* Lam. stem bark extract showed that H-3 is the bioactive fraction in suppressing melanogenesis in B16F10 melanoma cells by reducing melanin content and inhibiting cellular tyrosinase activity at a non-cytotoxic concentration (12  $\mu$ g/mL). The molecular analyses showed that H-3 exhibited multifunctional inhibitory activity against melanogenesis by direct suppression of *Mitf*, inhibition of the cAMP pathway, activation of the MAPK signaling pathways, melanosome degradation, as

well as scavenging the ROS in B16F10 melanoma cells. This study has provided substantial experimental evidence to support the potential use of *A. heterophyllum* stem bark as an active ingredient in skin-lightening cosmeceutical for the treatment of hyperpigmentation disorder on the molecular basis. It is hoped that when the *in vivo* studies of H-3 are clarified, the attractiveness and potential of H-3 from *A. heterophyllum* Lam. stem bark as active ingredients in skin-lightening cosmeceutical for the treatment of hyperpigmentation disorders can be substantially enhanced.

## ACKNOWLEDGEMENTS

The authors gratefully acknowledge the financial support from the Ministry of Education, Malaysia for the Fundamental Research Grant Scheme (FRGS), FP098-2019A (Reference code: FRGS/1/2019/STG04/UM/02/7).

## REFERENCES

- Alam, M.B., Ahmed, A., Motin, M.A., Kim, S. & Lee, S.H. 2018. Attenuation of melanogenesis by *Nymphaea nouchali* (Burm. f) flower extract through the regulation of cAMP/CREB/MAPKs/MITF and proteasomal degradation of tyrosinase. *Scientific Reports* 8(1): 13928.
- Alam, M.B., Bajpai, V.K., Lee, J., Zhao, P., Byeon, J.H., Ra, J.S., Majumder, R., Lee, J.S., Yoon, J.I., Rather, I.A., Park, Y.H., Kim, K., Na, M. & Lee, S.H. 2017. Inhibition of melanogenesis by jineol from *Scolopendra subspinipes mutilans* via MAP-Kinase mediated MITF downregulation and the proteasomal degradation of tyrosinase. *Scientific Reports* 7(1): 45858.
- Arung, E.T., Shimizu, K. & Kondo, R. 2011. *Artocarpus* plants as a potential source of skin whitening agents. *Natural Product Communications* 6(9): 1397-1402.
- Arung, E.T., Shimizu, K. & Kondo, R. 2006. Inhibitory effect of artocarpone from *Artocarpus heterophyllus* on melanin biosynthesis. *Biological and Pharmaceutical Bulletin* 29(9): 1966-1969.
- Bellei, B., Maresca, V., Flori, E., Pitisci, A., Larue, L. & Picardo, M. 2010. p38 regulates pigmentation via proteasomal degradation of tyrosinase. *Journal of Biological Chemistry* 285(10): 7288-7299.
- Bino, S.D., Duval, C. & Bernerd, F. 2018. Clinical and biological characterization of skin pigmentation diversity and its consequences on UV impact. *International Journal of Molecular Sciences* 19(9): 2668.
- Bult, C.J., Blake, J.A., Smith, C.L., Kadin, J.A., Richardson, J.E. & The Mouse Genome Database Group. 2019. Mouse genome database (MGD) 2019. *Nucleic Acids Research* 47(D1): D801-D806.
- Bustin, S.A., Benes, V., Garson, J.A., Hellems, J., Huggett, J., Kubista, M., Mueller, R., Nolan, T., Pfaffl, M.W., Shipley, G.L., Vandesompele, J. & Wittwer, C.T. 2009. The MIQE guidelines: Minimum information for publication of quantitative real-time PCR experiments. *Clinical Chemistry* 55(4): 611-622.
- Carlson, J.A., Linette, G.P., Aplin, A., Ng, B. & Slominski, A. 2007. Melanocyte receptors: Clinical implications and therapeutic relevance. *Dermatologic Clinics* 25(4): 541-557.
- Chaikul, P., Lourith, N. & Kanlayavattanakul, M. 2017. Antimelanogenesis and cellular antioxidant activities of rubber (*Hevea brasiliensis*) seed oil for cosmetics. *Industrial Crops and Products* 108: 56-62.
- Chiang, H.M., Chien, Y.C., Wu, C.H., Kuo, Y.H., Wu, W.C., Pan, Y.Y., Su, Y.H. & Wen, K.C. 2014. Hydroalcoholic extract of *Rhodiola rosea* L. (Crassulaceae) and its hydrolysate inhibit melanogenesis in B16F0 cells by regulating the CREB/MITF/tyrosinase pathway. *Food and Chemical Toxicology* 65: 129-139.
- Fu, Y.H., Guo, J.M., Xie, Y.T., Yu, X.M., Su, Q.T., Qiang, L., Kong, L.Y. & Liu, Y.P. 2020. Prenylated chromones from the fruits of *Artocarpus heterophyllus* and their potential anti-HIV-1 activities. *Journal of Agricultural and Food Chemistry* 68(7): 2024-2030.
- Glick, D., Barth, S. & Macleod, K.F. 2010. Autophagy: Cellular and molecular mechanisms. *The Journal of Pathology* 221(1): 3-12.
- Gotoh, I., Adachi, M. & Nishida, E. 2001. Identification and characterization of a novel MAP kinase kinase kinase, MLTK. *Journal of Biological Chemistry* 276(6): 4276-4286.
- Greenwood, M.P., Greenwood, M., Gillard, B.T., Chitra Devi, R. & Murphy, D. 2017. Regulation of cAMP responsive element binding protein 3-Like 1 (Creb3l1) expression by orphan nuclear receptor Nr4a1. *Frontiers in Molecular Neuroscience* 10: 413.
- Guo, Y.Q., Tang, G.H., Lou, L.L., Li, W., Zhang, B., Liu, B. & Yin, S. 2018. Prenylated flavonoids as potent phosphodiesterase-4 inhibitors from *Morus alba*: Isolation, modification, and structure-activity relationship study. *European Journal of Medicinal Chemistry* 144: 758-766.
- Hsiao, J.J. & Fisher, D.E. 2014. The roles of microphthalmia-associated transcription factor and pigmentation in melanoma. *Archives of Biochemistry and Biophysics* 563: 28-34.
- Hwang, Y., Lee, J., Jung, H.J., Ullah, S., Ko, J., Jeong, Y., Park, Y.J., Kang, M.K., Yun, H., Kim, M.S., Chun, P., Chung, H.Y. & Moon, H.R. 2022. A novel class of potent anti-tyrosinase compounds with antioxidant activity, 2-(substituted phenyl)-5-(trifluoromethyl)benzo[d]thiazoles: *in vitro* and *in silico* insights. *Antioxidants* 11(7): 1375.
- Jagtap, U. & Bapat, V. 2010. *Artocarpus*: A review of its traditional uses, phytochemistry and pharmacology. *Journal of Ethnopharmacology* 129(2): 142-166.
- Jeong, D., Park, S.H., Kim, M.H., Lee, S., Cho, Y.K., Kim, Y.A., Park, B.J., Lee, J., Kang, H. & Cho, J.Y. 2020. Anti-melanogenic effects of ethanol extracts of the leaves and roots of *Patrinia villosa* (Thunb.) juss through their inhibition of CREB and induction of ERK and autophagy. *Molecules* 25(22): 5375.
- Kanehisa, M. & Goto, S. 2000. KEGG: Kyoto encyclopedia of genes and genomes. *Nucleic Acids Research* 28(1): 27-30.
- Kawakami, A. & Fisher, D.E. 2017. The master role of microphthalmia-associated transcription factor in melanocyte and melanoma biology. *Laboratory Investigation* 97(6): 649-656.
- Keshet, Y. & Seger, R. 2010. The MAP kinase signaling cascades: A system of hundreds of components regulates a diverse array of physiological functions. In *MAP Kinase Signaling Protocols. Methods in Molecular Biology (Methods and Protocols)*, edited by Seger, R. Totowa: Humana Press.
- Kim, E.S., Park, S.J., Goh, M.J., Na, Y.J., Jo, D.S., Jo, Y.K., Shin, J.H., Choi, E.S., Lee, H.K., Kim, J.Y., Jeon, H.B., Kim, J.C. & Cho, D.H. 2014. Mitochondrial dynamics regulate melanogenesis through proteasomal degradation of MITF via ROS-ERK activation. *Pigment Cell & Melanoma Research* 27(6): 1051-1062.

- Kim, J., Choi, H., Cho, E.G. & Lee, T.R. 2014. FoxO3a is an antimelanogenic factor that mediates antioxidant-induced depigmentation. *Journal of Investigative Dermatology* 134(5): 1378-1388.
- Kim, J.Y., Kim, J., Ahn, Y., Lee, E.J., Hwang, S., Almurayshid, A., Park, K., Chung, H.J., Kim, H.J., Lee, S.H., Lee, M.S. & Oh, S.H. 2020. Autophagy induction can regulate skin pigmentation by causing melanosome degradation in keratinocytes and melanocytes. *Pigment Cell and Melanoma Research* 33(3): 403-415.
- Ko, F.N., Cheng, Z.J., Lin, C.N. & Teng, C.M. 1998. Scavenger and antioxidant properties of prenylflavones isolated From *Artocarpus heterophyllus*. *Free Radical Biology and Medicine* 25(2): 160-168.
- Ko, G.A., Shrestha, S. & Cho, S.K. 2018. *Sageretia thea* fruit extracts rich in methyl linoleate and methyl linolenate downregulate melanogenesis via the Akt/GSK3 $\beta$  signaling pathway. *Nutrition Research and Practice* 12(1): 3-12.
- Ko, G.A., Kang, H.R., Moon, J.Y., Ediriweera, M.K., Eum, S., Bach, T.T. & Cho, S.K. 2019. *Annona squamosa* L. leaves inhibit alpha-melanocyte-stimulating hormone ( $\alpha$ -MSH) stimulated melanogenesis via p38 signaling pathway in B16F10 melanoma cells. *Journal of Cosmetic Dermatology* 19(7): 1785-1792.
- Ko, H.H., Chiang, Y.C., Tsai, M.H., Liang, C.J., Hsu, L.F., Li, S.Y., Wang, M.C., Yen, F.L. & Lee, C.W. 2014. Eupafolin, a skin whitening flavonoid isolated from *Phyla nodiflora*, downregulated melanogenesis: Role of MAPK and Akt pathways. *Journal of Ethnopharmacology* 151(1): 386-393.
- Kumari, S., Thng, S.T.G., Verma, N.K. & Gautam, H.K. 2018. Melanogenesis inhibitors. *Acta Dermato-Venereologica* 98(9-10): 924-931.
- Kwon, S.H., Choi, H.R., Kang, Y.A. & Park, K.C. 2017. Depigmenting effect of resveratrol is dependent on FOXO3a activation without SIRT1 activation. *International Journal of Molecular Sciences* 18(6): 1213.
- Lee, C.C., Lin, C.N. & Jow, G.M. 2006. Cytotoxic and apoptotic effects of prenylflavonoid artonin B in human acute lymphoblastic leukemia cells. *Acta Pharmacologica Sinica* 27(9): 1165-1174.
- Lee, J.O., Kim, E., Kim, J.H., Hong, Y.H., Kim, H.G., Jeong, D., Kim, J., Kim, S.H., Park, C., Seo, D.B., Son, Y.J., Han, S.Y. & Cho, J.Y. 2018. Antimelanogenesis and skin-protective activities of *Panax ginseng* calyx ethanol extract. *Journal of Ginseng Research* 42(3): 389-399.
- Levy, C., Khaled, M. & Fisher, D.E. 2006. MITF: Master regulator of melanocyte development and melanoma oncogene. *Trends in Molecular Medicine* 12(9): 406-414.
- Li, J., Lin, Z., Tang, X., Liu, G., Chen, Y., Zhai, X., Huang, Q. & Cao, Y. 2020. Oxyresveratrol extracted from *Artocarpus heterophyllus* Lam. inhibits tyrosinase and age pigments *in vitro* and *in vivo*. *Food and Function* 11(7): 6595-6607.
- Li, Z., Lan, Y., Miao, J., Chen, X., Chen, B., Liu, G., Wu, X., Zhu, X. & Cao, Y. 2021. Phytochemicals, antioxidant capacity and cytoprotective effects of jackfruit (*Artocarpus heterophyllus* Lam.) axis extracts on HepG2 cells. *Food Bioscience* 41: 100933.
- Lin, C.N., Shieh, W.L., Ko, F.N. & Teng, C.M. 1993. Antiplatelet activity of some prenylflavonoids. *Biochemical Pharmacology* 45(2): 509-512.
- Liu, W.J., Ye, L., Huang, W.F., Guo, L.J., Xu, Z.G., Wu, H.L., Yang, C. & Liu, H.F. 2016. p62 links the autophagy pathway and the ubiquitin-proteasome system upon ubiquitinated protein degradation. *Cellular & Molecular Biology Letters* 21: 29.
- Ma, J., Guo, W. & Li, C. 2017. Ubiquitination in melanoma pathogenesis and treatment. *Cancer Medicine* 6(6): 1362-1377.
- Makbal, R., Villareal, M.O., Gadhi, C., Hafidi, A. & Isoda, H. 2020. *Argania spinosa* fruit shell extract-induced melanogenesis via cAMP signaling pathway activation. *International Journal of Molecular Sciences* 21(7): 2539.
- Matsui, M.S., Petris, M.J., Niki, Y., Karaman-Jurukovska, N., Muizzuddin, N., Ichihashi, M. & Yarosh, D.B. 2015. Omeprazole, a gastric proton pump inhibitor, inhibits melanogenesis by blocking ATP7A trafficking. *Journal of Investigative Dermatology* 135(3): 834-841.
- Miki, H., Setou, M., Kaneshiro, K. & Hirokawa, N. 2001. All kinesin superfamily protein, KIF, genes in mouse and human. *Proceedings of the National Academy of Sciences* 98(13): 7004-7011.
- Morrison, I.J., Zhang, J., Lin, J., Murray, J.E., Porter, R., Langat, M.K., Sadgrove, N.J., Barker, J., Zhang, G. & Delgoda, R. 2021. Potential chemopreventive, anticancer and anti-inflammatory properties of a refined artocarpin-rich wood extract of *Artocarpus heterophyllus* Lam. *Scientific Reports* 11(1): 6854.
- Nguyen, N.T., Nguyen, M.H.K., Nguyen, H.X., Bui, N.K.N. & Nguyen, M.T.T. 2012. Tyrosinase inhibitors from the wood of *Artocarpus heterophyllus*. *Journal of Natural Products* 75(11): 1951-1955.
- Ochiai, Y., Kaburagi, S., Okano, Y., Masaki, H., Ichihashi, M., Funasaka, Y. & Sakurai, H. 2008. A Zn(II)-glycine complex suppresses UVB-induced melanin production by stimulating metallothionein expression. *International Journal of Cosmetic Science* 30(2): 105-112.
- Oskoueian, E., Karimi, E., Noura, R., Ebrahimi, M., Shafaei, N. & Karimi, E. 2020. Nanoliposomes encapsulation of enriched phenolic fraction from pistachio hulls and its antioxidant, anti-inflammatory, and anti-melanogenic activities. *Journal of Microencapsulation* 37(1): 1-13.
- Pang, J.R., How, S.W., Wong, K.H., Lim, S.H., Phang, S.M. & Yow, Y.Y. 2022. Cholinesterase inhibitory activities of neuroprotective fraction derived from red alga *Gracilaria manilaensis*. *Fisheries and Aquatic Sciences* 25(2): 49-63.
- Parvez, S., Kang, M., Chung, H.S., Cho, C., Hong, M.C., Shin, M.K. & Bae, H. 2006. Survey and mechanism of skin depigmenting and lightening agents. *Phytotherapy Research* 20(11): 921-934.
- Pearson, D. 1976. *Chemical Analysis of Food*. Edinburg: Churchill Livingstone.
- Plensdorf, S. & Martinez, J. 2009. Common pigmentation disorders. *American Family Physician* 79(2): 109-116.
- Prakash, O., Kumar, R., Mishra, A. & Gupta, R. 2009. *Artocarpus heterophyllus* (Jackfruit): An overview. *Pharmacognosy Reviews* 3(6): 353-358.

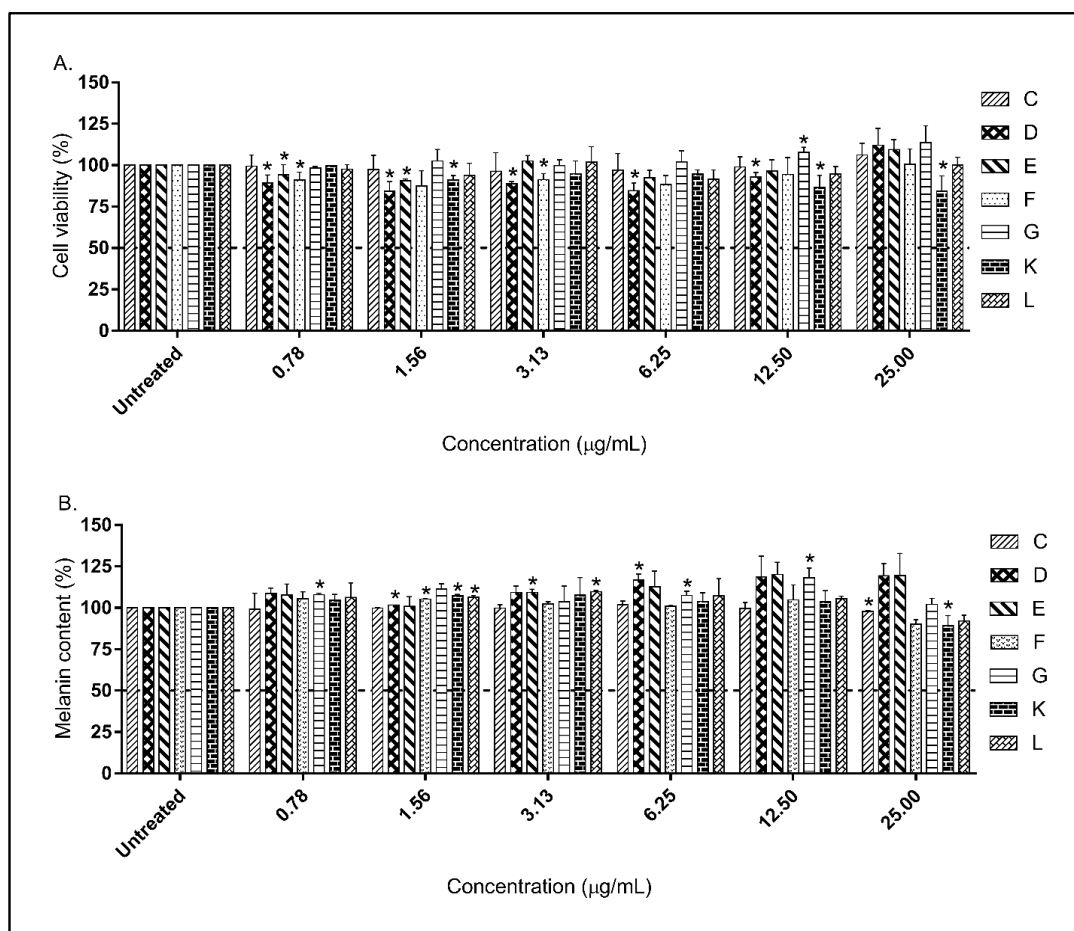
- Price, E.R., Horstmann, M.A., Wells, A.G., Weilbaecher, K.N., Takemoto, C.M., Landis, M.W. & Fisher, D.E. 1998.  $\alpha$ -melanocyte-stimulating hormone signaling regulates expression of microphthalmia, a gene deficient in Waardenburg syndrome. *Journal of Biological Chemistry* 273(49): 33042-33047.
- Ramli, A.N.M., Badruzaman, S.Z.S., Hamid, H.A. & Bhuyar, P. 2021. Antibacterial and antioxidative activity of the essential oil and seed extracts of *Artocarpus heterophyllus* for effective shelf-life enhancement of stored meat. *Journal of Food Processing and Preservation* 45(1): e14993.
- Roh, E., Jeong, I.Y., Shin, H., Song, S., Kim, N.D., Jung, S.H., Hong, J.T., Lee, S.H., Han, S.B. & Kim, Y. 2014. Downregulation of melanocyte-specific facultative melanogenesis by 4-hydroxy-3-methoxycinnamaldehyde acting as a cAMP antagonist. *Journal of Investigative Dermatology* 134(2): 551-553.
- Ryu, Y.B., Ha, T.J., Curtis-Long, M.J., Ryu, H.W., Gal, S.W. & Park, K.H. 2008. Inhibitory effects on mushroom tyrosinase by flavones from the stem barks of *Morus lhou* (S.) Koidz. *Journal of Enzyme Inhibition and Medicinal Chemistry* 23(6): 922-930.
- Saad, H.M., Tan, C.H., Lim, S.H., Manickam, S. & Sim, K.S. 2021. Evaluation of anti-melanogenesis and free radical scavenging activities of five *Artocarpus* species for cosmeceutical applications. *Industrial Crops and Products* 161: 113184.
- Sangkaew, O. & Yompakdee, C. 2020. Fermented unpolished black rice (*Oryza sativa* L.) inhibits melanogenesis via ERK, p38, and AKT phosphorylation in B16F10 melanoma cells. *Journal of Microbiology and Biotechnology* 30(8): 1184-1194.
- Seo, E.Y., Jin, S.P., Sohn, K.C., Park, C.H., Lee, D.H. & Chung, J.H. 2017. UCHL1 regulates melanogenesis through controlling MITF stability in human melanocytes. *Journal of Investigative Dermatology* 137(8): 1757-1765.
- Seo, G.Y., Ha, Y., Park, A.H., Kwon, O.W. & Kim, Y.J. 2019. *Leathesia difformis* extract inhibits  $\alpha$ -MSH-induced melanogenesis in B16F10 cells via down-regulation of CREB signaling pathway. *International Journal of Molecular Sciences* 20(3): 536.
- Solano, F., Briganti, S., Picardo, M. & Ghanem, G. 2006. Hypopigmenting agents: An updated review on biological, chemical and clinical aspects. *Pigment Cell Research* 19(6): 550-571.
- Sun, L., Guo, C., Yan, L., Li, H., Sun, J., Huo, X., Xie, X. & Hu, J. 2020. Syntenin regulates melanogenesis via the p38 MAPK pathway. *Molecular Medicine Reports* 22(2): 733-738.
- Taira, N., Katsuyama, Y., Yoshioka, M., Okano, Y. & Masaki, H. 2018. 3-O-Glyceryl-2-O-hexyl ascorbate suppresses melanogenesis by interfering with intracellular melanosome transport and suppressing tyrosinase protein synthesis. *Journal of Cosmetic Dermatology* 17(6): 1209-1215.
- Takizawa, T., Imai, T., Onose, J.I., Ueda, M., Tamura, T., Mitsumori, K., Izumi, K. & Hirose, M. 2004. Enhancement of hepatocarcinogenesis by kojic acid in rat two-stage models after initiation with N-bis(2-hydroxypropyl) nitrosamine or N-diethylnitrosamine. *Toxicological Sciences* 81(1): 43-49.
- Tan, C.H., Sim, D.S.Y., Lim, S.H., Mohd Mohidin, T.B., Mohan, G., Low, Y.Y., Kam, T.S. & Sim, K.S. 2022. Antiproliferative and microtubule-stabilizing activities of two iboga-vobasine bisindoles alkaloids from *Tabernaemontana corymbosa* in colorectal adenocarcinoma HT-29 cells. *Planta Medica* 88(14): 1325-1340.
- The UniProt, C. 2019. UniProt: A worldwide hub of protein knowledge. *Nucleic Acids Research* 47(D1): D506-D515.
- Tsatmali, M., Ancans, J. & Thody, A.J. 2002. Melanocyte function and its control by melanocortin peptides. *Journal of Histochemistry and Cytochemistry* 50(2): 125-133.
- Vázquez-González, Y., Ragazzo-Sánchez, J.A. & Calderón-Santoyo, M. 2020. Characterization and antifungal activity of jackfruit (*Artocarpus heterophyllus* Lam.) leaf extract obtained using conventional and emerging technologies. *Food Chemistry* 330: 127211.
- Villareal, M.O., Han, J., Ikuta, K. & Isoda, H. 2012. Mechanism of *Mitf* inhibition and morphological differentiation effects of hirsein A on B16 melanoma cells revealed by DNA microarray. *Journal of Dermatological Science* 67(1): 26-36.
- Wei, B.L., Weng, J.R., Chiu, P.H., Hung, C.F., Wang, J.P. & Lin, C.N. 2005. Antiinflammatory flavonoids from *Artocarpus heterophyllus* and *Artocarpus communis*. *Journal of Agricultural and Food Chemistry* 53(10): 3867-3871.
- Wu, M., Hemesath, T.J., Takemoto, C.M., Horstmann, M.A., Wells, A.G., Price, E.R., Fisher, D.Z. & Fisher, D.E. 2000. C-Kit triggers dual phosphorylations, which couple activation and degradation of the essential melanocyte factor Mi. *Genes and Development* 14(3): 301-312.
- Zheng, Y., Lee, E.H., Lee, S.Y., Lee, Y., Shin, K.O., Park, K. & Kang, I.J. 2023. *Morus alba* L. root decreases melanin synthesis via sphingosine-1-phosphate signaling in B16F10 cells. *Journal of Ethnopharmacology* 301: 115848.

\*Corresponding author; email: simkaeshin@um.edu.my

## S1. Primers of selected genes for qPCR analysis

Genes	Primer sequence	Amplicon size (base pair)	Reference
<i>Creb3l2</i>	F: 5'-GACTCTGAGGGCAGCTTGAG-3' R: 5'-AGATGTGGACAAGGCAGAGG-3'	111	-
<i>Creb3l3</i>	F: 5'-CTGACCCCAGCTCTCCATTA-3' R: 5'-ACTACGAGGAGGGGTGCCT-3'	95	-
<i>Map3k20</i>	F: 5'-ACACACATGTCCTTGTTGG-3' R: 5'-CAGGTTTCAGACACAGGGAGA-3'	77	-
<i>Mapk14</i>	F: 5'-GGACCTGAACAACATCGTGA-3' R: 5'-CCCTCGGAGGATCTGGTAGA-3'	79	-
<i>Mitf</i>	F: 5'-GTATGAACACGCACTCTCGA-3' R: 5'-GTAACGTATTGCCATTTGC-3'	135	Oskoucian et al. (2020)
<i>Tyr</i>	F: 5'-CGCCCTCTTTTGAAGTTTA-3' R: 5'-GAGCGGTATGAAAGGAACCA-3'	84	-
<i>Tyrp1</i>	F: 5'-CTTTCTCCCTTCTTACTGG-3' R: 5'-TCGTACTCTCCAAGGATTC-3'	163	Sangkaew & Yompakdee (2020)
<i>Dct</i>	F: 5'-TTATATCCTTCGAAACCAGGA-3' R: 5'-GGGAATGGATATCCGTCCTA-3'	176	Oskoucian et al. (2020)
<i>Gapdh</i>	F: 5'-TTGGCATTGTGGAAGGGCTC-3' R: 5'-ACCAGTGGATGCAGGGATGA-3'	134	Seo et al. (2019)

## S2. Biological assays for non-active fractions



Viability (A) and melanin content (B) of B16F10 melanoma cells after treatment with *A. heterophyllus* stem bark non-active fractions for 48 h. Values are expressed as the means  $\pm$  SD of three independent experiments. \* $p < 0.05$  indicates significant different from untreated control



S3. List of up- and down-regulated genes in B16F10 melanoma cells after treatment with H-3 (12 µg/mL)

Gene symbol	Gene name	Biological process	Log <sub>10</sub> (FC)	Reference(s)
<i>Il6st</i>	Interleukin 6 signal transducer	Cell differentiation, cell population proliferation, homeostasis, immune system, protein and lipid metabolic process, response to stimulus, signaling, system development	2.05	Bult et al. (2019); Kumari et al. (2018)
<i>Map3k20</i>	Mitogen-activated protein kinase kinase kinase 20	Cell death, cellular component organization, protein metabolic process, respond to stimulus, signaling	2.04	Bult et al. (2019); Gotoh, Adachi & Nishida (2001); The UniProt (2019)
<i>Csnk2a2</i>	Casein kinase 2, alpha prime polypeptide	Cell death, protein metabolic process, response to stimulus, signaling	1.49	Bult et al. (2019); The UniProt (2019); Villareal et al. (2012)
<i>Tpr</i>	Translocated promoter region	Cellular component organization, establishment of localization, nucleic acid-templated transcription, protein metabolic process, response to stimulus, signalling	1.45	Bult et al. (2019); Makbal et al. (2020)
<i>Gnao</i>	Guanine nucleotide binding protein, alpha O	Establishment of localization, response to stimulus, signaling	1.23	Bult et al. (2019); Kanehisa & Goto (2000)
<i>Mtfr2</i>	Mitochondrial fission regulator 2	Cellular component organization	1.20	Bult et al. (2019); Kumari et al. (2018)
<i>Sqstm1</i>	Sequestosome 1	Cell death, cell differentiation, cell population proliferation, cellular component organization, establishment of localization, homeostasis, immune system process, nucleic acid-templated transcription, protein metabolic process, response to stimulus, signaling	1.16	Bult et al. (2019); Jeong et al. (2020); Liu et al. (2016)
<i>Ulk1</i>	Unc-51 like kinase 1	Cell death, cell differentiation, cellular component organization, establishment of localization, protein metabolic process, response to stimulus, signaling, system development	1.16	Bult et al. (2019); Jeong et al. (2020)
<i>Uchl1os</i>	Ubiquitin carboxy-terminal hydrolase L1, opposite strand	Protein metabolic process, response to stimulus	1.15	Bult et al. (2019); Seo et al. (2017)
<i>Csnk1a1</i>	Casein kinase 1, alpha 1	Protein metabolic process, and response to stimulus, signaling	1.10	Bult et al. (2019); Villareal et al. (2012)
<i>Foxo3</i>	<i>Gpr143</i>	Cell death, cell differentiation, cell population proliferation, homeostasis, immune system, nucleic acid-templated transcription, protein metabolic process, response to stimulus, signaling, system development	1.10	Bult et al. (2019); Kim et al. (2014)

<i>Mapk14</i>	Mitogen-activated protein kinase 14	Cell death, cell population proliferation, cell differentiation, cellular component organization, establishment of localization, homeostasis, immune system, nucleic acid-templated transcription, protein and lipid metabolic process, response to stimulus, signaling, system development	1.01	Bult et al. (2019); Keshet & Seger (2010); The UniProt (2019)
<i>Creb3l1</i>	cAMP responsive element binding protein 3-like 1	Cell death, Cell differentiation, cellular component organization, establishment of localization, nucleic acid-templated transcription, response to stimulus, signaling, system development	-1.07	Bult et al. (2019); Greenwood et al. (2017); Kanehisa & Goto (2000)
<i>Fzd3</i>	Frizzled class receptor 3	Cell death, cell population proliferation, cell differentiation, cellular components organization, response to stimulus, signaling, system development	-1.07	Bult et al. (2019); Carlson et al. (2007); Kanehisa & Goto (2000)
<i>Gpr143</i>	<i>Mapk14</i>	Melanosome organization, melanosome localization, melanosome transport, response to stimulus, signaling	-1.14	Bult et al. (2019); Makbal et al. (2020)
<i>Prkca</i>	Protein kinase C, alpha	Cell death, cell differentiation, cell population proliferation, cellular component organization, establishment of localization, homeostasis, immune system, protein metabolic process, response to stimulus, signaling, system development	-1.23	Bult et al. (2019); Kanehisa & Goto (2000)
<i>Creb3l2</i>	cAMP responsive element binding protein 3-like 2	Cell differentiation, cellular component organization, establishment of localization, nucleic acid-templated transcription, response to stimulus, signaling, system development	-1.29	Bult et al. (2019); Kanehisa & Goto (2000); Villareal et al. (2012)
<i>Sorbs3</i>	Sorbin and SH3 domain containing 3	Cellular component organization, nucleic acid-templated transcription, response to stimulus, signaling	-1.29	Bult et al. (2019); Villareal et al. (2012)
<i>Creb3l3</i>	cAMP responsive element binding protein 3-like 3	Nucleic acid-templated transcription, response to stimulus, signaling	-1.33	Bult et al. (2019); Glick, Barth & Macleod (2010); Kanehisa & Goto (2000)
<i>Calm1</i>	Calmodulin-1	Establishment of localization, homeostasis, protein metabolic process, response to stimulus	-1.42	Bult et al. (2019); Kanehisa & Goto (2000)

<i>Tyr</i>	Tyrosinase	Cell population proliferation, immune system process, respond to stimulus, system development, melanin biosynthesis, pigmentation,	-1.43	Bult et al. (2019); The UniProt (2019)
<i>Trpm1</i>	Transient receptor potential cation channel subfamily M, member 1	Cell differentiation, cellular component organization, establishment of localization, homeostasis, response to stimulus, signaling, system development	-1.64	Bult et al. (2019); Ma, Guo & Li (2017)
<i>Kif6</i>	Kinesin family member 6	Microtubule-based movement	-1.65	Miki et al. (2001); The UniProt (2019)
<i>Plcb1</i>	Phospholipase C, beta 1	Carbohydrate derivative metabolism, cell differentiation, cellular component organization, establishment of localization, homeostasis, immune system, nucleic acid-templated transcription, protein and lipid metabolic process, response to stimulus, signaling, system development	-1.70	Bult et al. (2019); Kanehisa & Goto (2000)
<i>Mitf</i>	Melanogenesis associated transcription factor	Cell death, cell population proliferation, cell differentiation, melanocyte differentiation, pigmentation, cellular component organization, immune system, nucleic acid-templated transcription, response to stimulus, signaling, system development	-1.77	Bult et al. (2019); Makbal et al. (2020); Villareal et al. (2012)
<i>Atp7b</i>	ATPase, Cu <sup>++</sup> transporting, beta polypeptide	Establishment of localization, homeostasis, protein metabolic process, respond to stimulus, system development	-1.78	Bult et al. (2019); Matsui et al. (2015)
<i>Atf1</i>	Activating transcription factor 1	Cell differentiation, cellular component organization, nucleic acid-templated transcription, system development	-1.84	Bult et al. (2019); Kawakami & Fisher (2017); Roh et al. (2014)
<i>Fzd6</i>	Frizzled class receptor 6	Cell population proliferation, nucleic acid-templated transcription, response to stimulus, signaling, system development	-2.26	Bult et al. (2019); Carlson et al. (2007); Kanehisa & Goto (2000)
<i>Mlph</i>	Melanophilin	Melanocyte differentiation, melanosome localization, pigmentation, protein targeting	-2.76	Lee et al. (2018); The UniProt (2019)

---

#### S4. Experimental

##### Pesticide Residue Testing

The identification of pesticide components from *A. heterophyllus* Lam. stem bark extract was performed at Alpha Testing Labs, Malaysia using Bruker Scion 456 GC with a triple quadrupole mass spectrometer equipped with MEGA-5MS fused silica capillary column (length: 30 m, inner diameter: 0.25 mm, film thickness: 0.25 mm). The carrier gas used was hydrogen with a flow rate of 1 mL/min. The injection was conducted in splitless mode at a temperature of 250 °C. The initial GC column temperature was 50 °C and then was raised to 320 °C at the rate of 10 °C/min. The MS was operated in the electron ionization mode at 70 Ev. The ion source temperature for MS was 250 °C with a transfer line temperature of 300 °C. The

mass spectra scan mode was range from 45-450 m/z. The peaks were identified by comparing with their mass fragmentation pattern from the NIST17 library.

##### Proximate Composition

The proximate analysis of *A. heterophyllus* Lam. stem bark extract was performed at Alpha Testing Labs, Malaysia. In accordance with Pearson (1976) the carbohydrate content was determined by differential summation of combined protein, fat, ash, crude fibre, and moisture. Fat content was determined using Soxhlet extraction, followed by gravimetric quantification of the extract and protein content was determined using the Kjeldahl method for total nitrogen multiply by a factor of 6.25.

#### S5. Pesticide residue analysis

Pesticide	Result
2,6-Dichlorobenzamide	ND <sup>1</sup>
4,4-Dichlorobenzophenone	ND <sup>1</sup>
a-BHC	ND <sup>1</sup>
Acetochlor	ND <sup>1</sup>
Acrinathrin	ND <sup>1</sup>
a-Ebdosulfan	ND <sup>1</sup>
Alachlor	ND <sup>1</sup>
Allethrin 1	ND <sup>1</sup>
Allethrin 2	ND <sup>1</sup>
Ametryn	ND <sup>1</sup>
Amitraz	ND <sup>1</sup>
Anilofos	ND <sup>1</sup>
Atrazine	ND <sup>1</sup>
Azaconazole	ND <sup>1</sup>
Azamethiphos	ND <sup>1</sup>
Azinphos-ethyl	ND <sup>1</sup>
Azinphos-methyl	ND <sup>1</sup>
Azoxystrobin	ND <sup>1</sup>
b-BHC	ND <sup>1</sup>
b-Endosulfan	ND <sup>1</sup>
Benfluralin	ND <sup>1</sup>
Benfuresate	ND <sup>1</sup>
Benalaxyl	ND <sup>1</sup>
Benthiocarb	ND <sup>1</sup>
Bifenox	ND <sup>1</sup>
Bifenazate	ND <sup>1</sup>
Bifenthrin	ND <sup>1</sup>
Bioresmethrin	ND <sup>1</sup>
Biromuconazole 2	ND <sup>1</sup>
Biphenyl	ND <sup>1</sup>
Bitertanol 1	ND <sup>1</sup>

Bitertanol 2	ND <sup>1</sup>
Bromacil	ND <sup>1</sup>
Bromobutide	ND <sup>1</sup>
Bromophos	ND <sup>1</sup>
Bromopropylate	ND <sup>1</sup>
Bromuconazole 1	ND <sup>1</sup>
Buprofezin	ND <sup>1</sup>
Butachlor	ND <sup>1</sup>
Butafenacil	ND <sup>1</sup>
Butamifos	ND <sup>1</sup>
Butylate	ND <sup>1</sup>
Cadusafos	ND <sup>1</sup>
Cafenstrole	ND <sup>1</sup>
Captafol	ND <sup>1</sup>
Captan	ND <sup>1</sup>
Carbetamide	ND <sup>1</sup>
Carbophenothion	ND <sup>1</sup>
Carfentrazone-ethyl	ND <sup>1</sup>
Chinomethionat	ND <sup>1</sup>
Chlorfenapyr	ND <sup>1</sup>
Chlorfenson	ND <sup>1</sup>
Chlormephos	ND <sup>1</sup>
Clomeprop	ND <sup>1</sup>
Chlomethoxynil	ND <sup>1</sup>
Chloridazon	ND <sup>1</sup>
Chlornitrofen	ND <sup>1</sup>
Chlorobenzilate	ND <sup>1</sup>
Chlorothalonil	ND <sup>1</sup>
Chlorpropham	ND <sup>1</sup>
Chloropropylate	ND <sup>1</sup>
Chlorpyrifos	ND <sup>1</sup>
Chlorpyrifos-methyl	ND <sup>1</sup>
Chlorthiophos	ND <sup>1</sup>
Cinmethylin	ND <sup>1</sup>
Crimidine	ND <sup>1</sup>
Cyanazine	ND <sup>1</sup>
Cyanofenphos	ND <sup>1</sup>
Cyanophos	ND <sup>1</sup>
Cyflufenamid	ND <sup>1</sup>
Cyfluthrin 1	ND <sup>1</sup>
Cyfluthrin 2	ND <sup>1</sup>
Cyfluthrin 3	ND <sup>1</sup>
Cyfluthrin 4	ND <sup>1</sup>
Cyhalofop butyl	ND <sup>1</sup>
Cyhalothrin 1	ND <sup>1</sup>
Cyhalothrin 2	ND <sup>1</sup>
Cypermethrin 1	ND <sup>1</sup>
Cypermethrin 2	ND <sup>1</sup>

Cypermethrin 3	ND <sup>1</sup>
Cypermethrin 4	ND <sup>1</sup>
Cyproconazole	ND <sup>1</sup>
Cyprodinyl	ND <sup>1</sup>
d-BHC	ND <sup>1</sup>
Deltamethrin	ND <sup>1</sup>
Demeton-S-methyl	ND <sup>1</sup>
Desmedipham	ND <sup>1</sup>
Dialifos	ND <sup>1</sup>
Diazinon	ND <sup>1</sup>
Dibrom	ND <sup>1</sup>
Dichlobenil	ND <sup>1</sup>
Diclobutrazol	ND <sup>1</sup>
Diethofencarb	ND <sup>1</sup>
Dichlofenthion	ND <sup>1</sup>
Dichlofluanid	ND <sup>1</sup>
Dichlofluanid metabolite	ND <sup>1</sup>
Dicloran	ND <sup>1</sup>
Dichlorvos	ND <sup>1</sup>
Dicrotophos	ND <sup>1</sup>
Difenoconazol 1	ND <sup>1</sup>
Difenoconazol 2	ND <sup>1</sup>
Diffufenican	ND <sup>1</sup>
Dimepiperate	ND <sup>1</sup>
Dimethametryn	ND <sup>1</sup>
Dimethenamid	ND <sup>1</sup>
Dimethipin	ND <sup>1</sup>
Dimethoate	ND <sup>1</sup>
Dimethomorph 1	ND <sup>1</sup>
Dimethomorph 2	ND <sup>1</sup>
Dimethylvinphos 1	ND <sup>1</sup>
Dimethylvinphos 2	ND <sup>1</sup>
Diniconazole	ND <sup>1</sup>
Dioxabenzofos	ND <sup>1</sup>
Dioxathion	ND <sup>1</sup>
Diphenamid	ND <sup>1</sup>
Diphenylamine	ND <sup>1</sup>
Disulfoton	ND <sup>1</sup>
Ditalimfos	ND <sup>1</sup>
Dithiopyr	ND <sup>1</sup>
Edifenphos	ND <sup>1</sup>
Esprocarb	ND <sup>1</sup>
Ethion	ND <sup>1</sup>
Ethofenprox	ND <sup>1</sup>
Ethoprophos	ND <sup>1</sup>
Ethychlozate	ND <sup>1</sup>
Ethyl dipropylthiocarbamate	ND <sup>1</sup>
Etobenzanid	ND <sup>1</sup>

Etoazole	ND <sup>1</sup>
Etridiazole	ND <sup>1</sup>
Etrimfos	ND <sup>1</sup>
Fenamiphos	ND <sup>1</sup>
Fenarimol	ND <sup>1</sup>
Fenbuconazole	ND <sup>1</sup>
Fenchlorphos	ND <sup>1</sup>
Fenitrothion	ND <sup>1</sup>
Fenothiocarb	ND <sup>1</sup>
Fenoxanil	ND <sup>1</sup>
Fenoxaprop ethyl	ND <sup>1</sup>
Fenoxycarb	ND <sup>1</sup>
Fenpropathrin	ND <sup>1</sup>
Fenpropimorph	ND <sup>1</sup>
Fensulfothion	ND <sup>1</sup>
Fenthion	ND <sup>1</sup>
Fenvalerate 1	ND <sup>1</sup>
Fenvalerate 2	ND <sup>1</sup>
Ferimzone	ND <sup>1</sup>
Fipronil	ND <sup>1</sup>
Fluacrypyrim	ND <sup>1</sup>
Flucythrinate 1	ND <sup>1</sup>
Flucythrinate 2	ND <sup>1</sup>
Fludioxunil	ND <sup>1</sup>
Flumioxazin	ND <sup>1</sup>
Fluquinconazole	ND <sup>1</sup>
Flusilazole	ND <sup>1</sup>
Flusilazole metabolite	ND <sup>1</sup>
Fluthiacet-methyl	ND <sup>1</sup>
Flutolanil	ND <sup>1</sup>
Fluvalinate 1	ND <sup>1</sup>
Fluvalinate 2	ND <sup>1</sup>
Folpet	ND <sup>1</sup>
Fonofos	ND <sup>1</sup>
Formothion	ND <sup>1</sup>
Fosthiazate 1	ND <sup>1</sup>
Fosthiazate 2	ND <sup>1</sup>
Furametpyr	ND <sup>1</sup>
Furametpyr metabolite	ND <sup>1</sup>
Halfenprox	ND <sup>1</sup>
Hexaconazole	ND <sup>1</sup>
Hymexazol	ND <sup>1</sup>
Indanofan	ND <sup>1</sup>
Indoxacarb	ND <sup>1</sup>
Iprobenfos	ND <sup>1</sup>
Iprodione	ND <sup>1</sup>
Iprodione metabolite	ND <sup>1</sup>
Isazophos	ND <sup>1</sup>

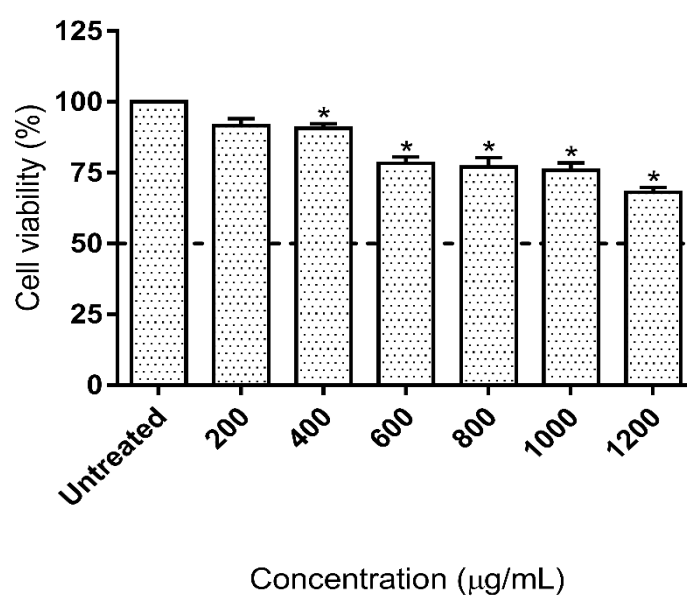


Isocarbophos	ND <sup>1</sup>
Isofenphos	ND <sup>1</sup>
Isoprothiolane	ND <sup>1</sup>
Isoxathion	ND <sup>1</sup>
Kresoxim-methyl	ND <sup>1</sup>
Lenacil	ND <sup>1</sup>
Leptophos	ND <sup>1</sup>
Lindane	ND <sup>1</sup>
Malathion	ND <sup>1</sup>
MCPB ethyl ester	ND <sup>1</sup>
Mecarbam	ND <sup>1</sup>
Mefenacet	ND <sup>1</sup>
Mepronil	ND <sup>1</sup>
Metalaxyl	ND <sup>1</sup>
Methacrifos	ND <sup>1</sup>
Methidathion	ND <sup>1</sup>
Methyl parathion	ND <sup>1</sup>
Methoprene 1	ND <sup>1</sup>
Methoprene 2	ND <sup>1</sup>
Metolaclor	ND <sup>1</sup>
Metominostrobin E	ND <sup>1</sup>
Metribuzin	ND <sup>1</sup>
Mexinphos	ND <sup>1</sup>
Molinate	ND <sup>1</sup>
Monocrotophos	ND <sup>1</sup>
Myclobutanil	ND <sup>1</sup>
Napropamide	ND <sup>1</sup>
Nereistoxin oxalate	ND <sup>1</sup>
Nitrofen	ND <sup>1</sup>
Nitralin	ND <sup>1</sup>
Omethoate	ND <sup>1</sup>
Oxabetrinil	ND <sup>1</sup>
Oxadiazon	ND <sup>1</sup>
Oxadixyl	ND <sup>1</sup>
Paclobutrazol	ND <sup>1</sup>
Parathion	ND <sup>1</sup>
Penconazole	ND <sup>1</sup>
Pendimethalin	ND <sup>1</sup>
Pentoxazone	ND <sup>1</sup>
Permethrin 1	ND <sup>1</sup>
Permethrin 2	ND <sup>1</sup>
Phenothiol	ND <sup>1</sup>
Phenothrin 1	ND <sup>1</sup>
Phenothrin 2	ND <sup>1</sup>
Phenthoate	ND <sup>1</sup>
Phosmet	ND <sup>1</sup>
Phosphamidon 1	ND <sup>1</sup>
Phosphamidon 2	ND <sup>1</sup>

Phorate	ND <sup>1</sup>
Phosalone	ND <sup>1</sup>
Phthalide	ND <sup>1</sup>
Piperophos	ND <sup>1</sup>
Piperonyl butoxide	ND <sup>1</sup>
Pirimiphos-methyl	ND <sup>1</sup>
Pretilachlor	ND <sup>1</sup>
Procymidone	ND <sup>1</sup>
Profenofos	ND <sup>1</sup>
Prohydrojasmon	ND <sup>1</sup>
Prometryn	ND <sup>1</sup>
Propachlor	ND <sup>1</sup>
Propanil	ND <sup>1</sup>
Propaphos	ND <sup>1</sup>
Propargite 1	ND <sup>1</sup>
Propargite 2	ND <sup>1</sup>
Propiconazole 1	ND <sup>1</sup>
Propiconazole 2	ND <sup>1</sup>
Propyzamide	ND <sup>1</sup>
Prothiofos	ND <sup>1</sup>
Pyiminobac-methyl (Z)	ND <sup>1</sup>
Pyraclufos	ND <sup>1</sup>
Pyraflufen-ethyl	ND <sup>1</sup>
Pyrazophos	ND <sup>1</sup>
Pyrazoxyfen	ND <sup>1</sup>
Pyributicarb	ND <sup>1</sup>
Pyridaben	ND <sup>1</sup>
Pyridaphenthion	ND <sup>1</sup>
Pyrifenox 1	ND <sup>1</sup>
Pyrifenox	ND <sup>1</sup>
Pyrimethanil	ND <sup>1</sup>
Pyrimidifen	ND <sup>1</sup>
Pyriminobac-methyl (E)	ND <sup>1</sup>
Pyriproxyfen	ND <sup>1</sup>
Pyroquilon	ND <sup>1</sup>
Quinalphos	ND <sup>1</sup>
Quintozene	ND <sup>1</sup>
Quizalofop-ethyl	ND <sup>1</sup>
Silafluofen	ND <sup>1</sup>
Simazine	ND <sup>1</sup>
Simeconazole	ND <sup>1</sup>
Simetryn	ND <sup>1</sup>
Spirodiclofen	ND <sup>1</sup>
Sulfotep	ND <sup>1</sup>
Sulprofos	ND <sup>1</sup>
Swep	ND <sup>1</sup>
Tebuconazole	ND <sup>1</sup>
Tebufenpyrad	ND <sup>1</sup>

Tecnazene	ND <sup>1</sup>
Tefluthrin	ND <sup>1</sup>
Terbacil	ND <sup>1</sup>
Terbucarb	ND <sup>1</sup>
Terbufos	ND <sup>1</sup>
Tetrachlorvinphos	ND <sup>1</sup>
Tetradifon	ND <sup>1</sup>
Tetramethrin 1	ND <sup>1</sup>
Tetramethrin 2	ND <sup>1</sup>
Thenylchlor	ND <sup>1</sup>
Thifluzamide	ND <sup>1</sup>
Thiocyclam	ND <sup>1</sup>
Thiometon	ND <sup>1</sup>
Tolclofos-methyl	ND <sup>1</sup>
Tolfenpyrad	ND <sup>1</sup>
Tolyfluamid	ND <sup>1</sup>
Tolyfluamid metabolite	ND <sup>1</sup>
Triadimefon	ND <sup>1</sup>
Triadimenol 1	ND <sup>1</sup>
Triadimenol 2	ND <sup>1</sup>
Triazophos	ND <sup>1</sup>
Trichlamide	ND <sup>1</sup>
Trichlorfon	ND <sup>1</sup>
Trifloxystrobin	ND <sup>1</sup>
Trifluralin	ND <sup>1</sup>
Uniconzole	ND <sup>1</sup>
Vinclozolin	ND <sup>1</sup>
Xylylcarb	ND <sup>1</sup>

Pesticide screening on *A. hetrophyllus* Lam. stem bark was carried out using GC/MS analysis. ND: not detected; <sup>1</sup>Limit of quantification 0.1 mg/kg



S6. Cell viability of kojic acid at 200-1200 µg/mL. Effect of kojic acid on the cell viability of B16F10 melanoma cells at concentration 200-1200 µg/mL. Values are represented as the means ± SD of three independent experiments. \* $p < 0.05$  indicates significant different from untreated control